Joint Space-Time Coherent Vibration Driven Conformational Transitions in a Single Molecule

Shaowei Li (李绍巍),[1] Siyu Chen (陈思宇),[1] Jie Li,[2] Ruqian Wu,[1,2,†] and W. Ho[1,3,*]
[1]Department of Physics and Astronomy, University of California, Irvine, California 92697-4575, USA
[2]State Key Laboratory of Surface Physics and Key Laboratory of Computational Physical Sciences, Fudan University, Shanghai, China 200433
[3]Department of Chemistry, University of California, Irvine, California 92697-2025, USA
(Received 24 July 2017; revised manuscript received 9 September 2017; published 26 October 2017)

We report single-molecule conformational transitions with joint angstrom-femtosecond resolution by irradiating the junction of a scanning tunneling microscope with femtosecond laser pulses. An isolated pyrrolidine molecule adsorbed on a Cu(001) surface undergoes reversible transitions between two conformational states. The transition rate decays in time and exhibits sinusoidal oscillations with periods of specific molecular vibrations. The dynamics of this transition depends sensitively on the molecular environment, as exemplified by the effects of another molecule in proximity.

DOI: 10.1103/PhysRevLett.119.176002

Femtosecond lasers have been used to reveal quantum beat phenomena in the time domain, leading to a valuable understanding of the energies and dynamics of various states in molecular and condensed matter systems [1]. By tailoring the amplitude and phase for each pair of laser pulses, quantum-mechanical interferences between different excited states can be modified and monitored [2]. This leads to the fascinating possibility of coherent control of molecular reactions by choosing the excitation pathway that maximizes the yield of a desired product. One hurdle in achieving this goal arises from the inhomogeneity in an ensemble of molecules [3,4]. Each molecule could be influenced by its local environment and requires a specific driving pulse profile to control its behavior. A new approach with angstrom (Å) spatial resolution and femtosecond (fs) temporal sensitivity would avoid the ensemble average and probe the coherent response of an individual molecule.

The pump-probe technique has been used to probe the coherent properties of solid state matter by monitoring changes in the linear reflectivity [5,6], the generation of second harmonic or sum frequency light [7–10], and the emission of electrons [11]. Because of the diffraction limited spatial resolution, these studies can only probe the homogeneous properties of the ensemble. The advancement of single-molecule techniques has enabled the detection of the absorption [12] and fluorescence [13] of individual molecules embedded in molecular solids. Furthermore, the spatial resolution has been enhanced by at least a factor of 10 through the invention of the super-resolved fluorescence microscopy [14,15] and near-field optical microscopy [16–18]. Still, the attainment of atomic-scale resolution remains elusive. The combination of laser with a scanning tunneling microscope (STM) can overcome this limitation. The efficiency of laser-induced electron transfer to a single molecule adsorbed on a solid surface was found to vary spatially within the molecule [19,20]. Spin coherence excited by circularly polarized light in GaAs quantum wells has been detected by the STM with ~1 nm resolution [21]. Most recently, the coherent vibration of single adsorbed molecules was detected by monitoring the photoinduced rectification of the tunneling current in the STM irradiated with terahertz laser pulses [22]. However, the possibility of a single-molecule transformation driven by coherent electronic or vibrational excitation has yet to be demonstrated.

In this Letter, we demonstrate the coherent vibration driven conformational changes of a single molecule using the combination of a femtosecond laser with a STM. The light-induced changes in the STM tunneling conductance are probed in the time domain and associated with reversible transitions between two structural states of a pyrrolidine adsorbed on a Cu(001) surface at 8.6 K. The output of the femtosecond laser consists of 35 fs pulses at a 5 GHz repetition rate, 820 nm wavelength, and bandwidth of 25 nm. The experimental approach is shown schematically in Fig. 1(a), and additional details are described in Supplemental Material [23]. We show that the laser-induced structural transition rate exhibits coherent oscillations with a dominant vibrational frequency and decay time, implicating this vibrational coordinate as the reaction coordinate for the conformational change.

The reversible transition between the two structural states of pyrrolidine (I and II) is shown schematically in Fig. 1(b). In a previous study without light, this conformational change in pyrrolidine was shown to be driven by its vibrations excited by inelastic tunneling electrons [34]. At a low sample bias without laser excitation, both molecular conformational states can be captured in topographic images, as shown in Fig. 1(c) and cross-sectional cuts in Fig. 1(d). The transition between these two states can be monitored at a fixed sample bias by changes in the

tunneling gap while maintaining a constant current (feedback on) or by changes in the tunneling current at a fixed gap (feedback off). Traces of the time-dependent changes in the tunneling gap, Δz, are shown in Fig. 1(e). In the absence of light, the rate of structural transition can be decreased by lowering the energy of the tunneling electrons as determined by the sample bias.

The transition rate significantly increases for the monomer when femtosecond laser pulses irradiate the STM junction. A further increase in the transition rate is observed when two molecules are in close proximity, noted as a dimer. Additionally, four distinct levels (I–IV) are observed when the STM tip is positioned over the middle of the dimer where the four possible combinations of states of the two molecules are excited and monitored. The residence times in either state I or II, obtained from the time traces, are exponentially distributed, as shown in Supplemental Material [23]. The transition rate can then be taken as the number of cycles of down and up changes in Δz per unit time. The delay scan is taken by counting the transition rate at different delay times between a pair of time-correlated pulses. In Fig. 1(f), the transition rate was measured along 17 locations above the molecule. The observed spatial variations in Fig. 1(g) are from a convolution of resolutions from the laser excitation and the STM probe. Since electron tunneling is confined to the Å scale, the spatial variations measured within the molecule in Fig. 1(g) imply atomic-scale resolution in the femtosecond laser excitation.

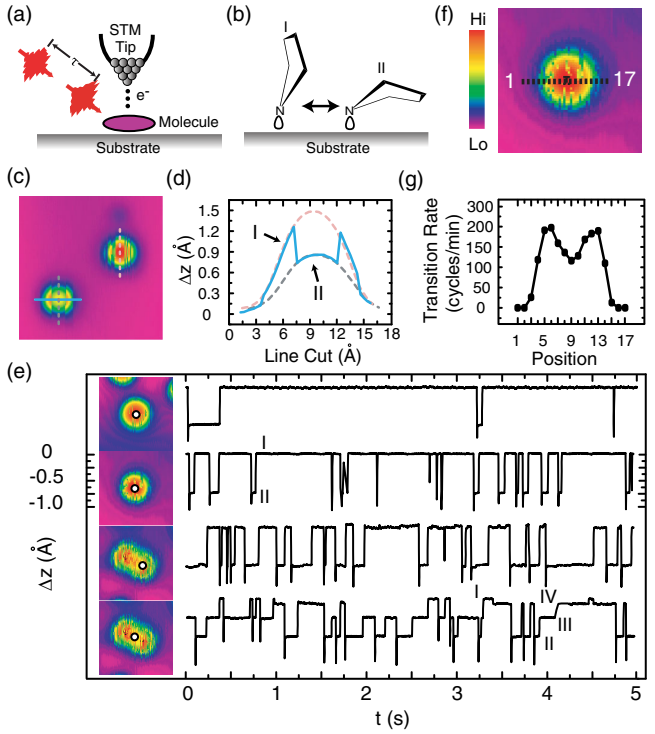

FIG. 1. (a) Schematic diagram of the STM junction illuminated by pairs of phase-correlated femtosecond laser pulses. (b) Reversible transitions between two structural states I and II for pyrrolidine on Cu(001). (c) Topographic images revealing the two states. (d) Vertical line cut across state I of the upper molecule [red dashed lines in (c) and (d)]; vertical line cut (black dashed line of state II) and horizontal line cut [blue solid lines in (c) and (d) showing I to II and II to I transitions] across the lower molecule. (e) Topographic images and corresponding time traces of changes in the tunneling gap (Δz) recorded over positions marked by a circular symbol, from top to bottom: isolated pyrrolidine molecule without light; isolated pyrrolidine irradiated by a laser; lower molecule in the dimer irradiated by a laser; center of the dimer with a laser. Tunneling gap set at 30 mV sample bias, 50 pA tunneling current, and with the feedback on. A transition cycle consists of I to II and back to I. (f) Topographic image showing the 17 locations where the transition rate was measured. (g) Transition rate obtained from Δz trace recorded for 300 s for the 17 locations.

Amplitude oscillations are observed in a delay scan of the femtosecond laser-induced transition rate with the tip positioned over the center of a monomer, as shown in Fig. 2(a). Control experiments at the bottom of Fig. 2(a) show a constant transition rate with continuous wave irradiation or in the absence of light. A fast Fourier transform (FFT) of the time delay scan in Fig. 2(a) reveals two peaks in the frequency domain as shown in Fig. 2(b). The delay scan from −3500 to +3500 fs can be fit by the sum of three parts in Eq. (1): a coherent signal R_{coh} of two exponentially decaying sinusoidal functions [Eq. (2)], a constant incoherent signal R_{inc} [Eq. (3)], and a Gaussian function R_{Gauss} [Eq. (4)]. The frequencies and relative amplitude for the sinusoidal functions in R_{coh} are obtained from the two peaks in the FFT spectrum in Fig. 2(b).

$$R = R_{\mathrm{coh}} + R_{\mathrm{inc}} + R_{\mathrm{Gauss}}, \tag{1}$$

$$R_{\mathrm{coh}} = \sum_{i=1}^{2} [A_i \sin(2\pi f_i \tau + \phi)] e^{-|\tau|/T}, \tag{2}$$

$$R_{\mathrm{inc}} = \mathrm{const}, \tag{3}$$

$$R_{\mathrm{Gauss}} = A e^{-\tau^2/(2\sigma^2)}. \tag{4}$$

The decay constant T of 1.30 ± 0.17 ps and phase ϕ of 90° are obtained from the fit by assuming the same values for both vibrations. The 6.9 THz vibration dominates the oscillations in the transition rate, as shown in Fig. 2(b), and similarly would determine the decay constant and phase. The additional small peak at 2.7 THz is responsible for the weak beating that can be seen in the delay scans shown in the insets in Fig. 2(a). The results of the delay scans are quantitatively robust for different monomers. The substrate atoms can be resolved by scanning at a reduced tunneling gap with a trapped H_2 molecule [24–30], as shown in Fig. 2(c), to reveal that the center of each molecule's topographic image coincides with a substrate surface atom. The 1.30 ± 0.17 ps decay time is approximately half the values measured for the

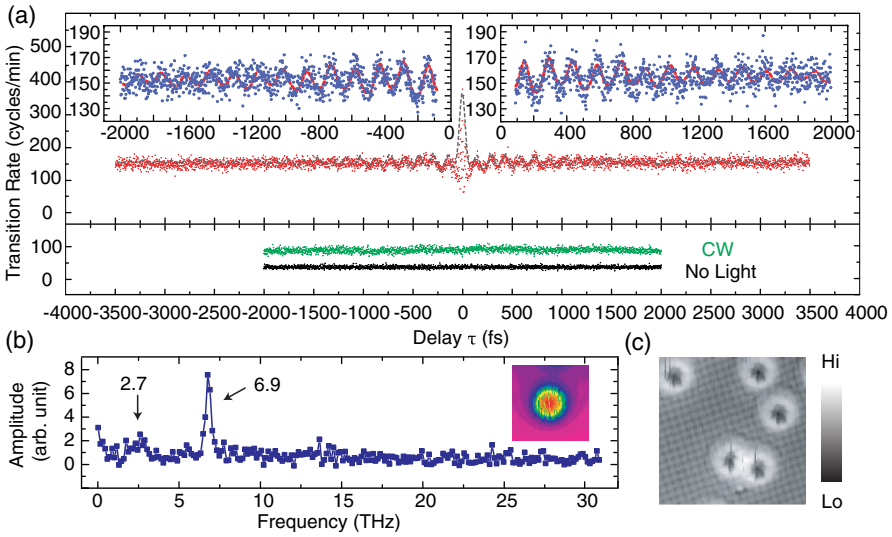

FIG. 2. (a) Delay scan (red dots, −3500 to +3500 fs in 2 fs steps) over the center of a monomer. The sign of the delay reflects the temporal order of the two pulses. The transition rate is determined from the sum of five passes, each pass with Δz trace recorded for 12 s at every delay, except one pass of 60 s at each delay for $|\tau| \leq 100$ fs. The black dashed line is the fit using Eq. (1). The two insets above (blue dots) show delay scans from the sum of ten passes; the same fit is shown. The green dots are the transition rate vs delay of the control measurement at the same total power of 1.5 mW of cw light at 820 nm (laser not mode locked). The black dots are for the transition rate in the dark vs delay, another control measurement. (b) Fourier transform of the data presented in (a), showing a dominant peak (145 ± 4 fs, 6.9 ± 0.2 THz, or 28.5 ± 0.7 meV) and a weak peak (365 ± 44 fs, 2.7 ± 0.3 THz, or 11.3 ± 1.4 meV). The uncertainty of the 6.9 THz peak is obtained from fitting the delay scan to only the dominant sinusoidal function at 6.9 THz. The uncertainty of the 2.7 THz peak is the step size in the FFT spectrum. The inset shows the topographic image of the molecule for all the data in this figure. (c) Topographic image taken in the dark with the gap set at 3 mV, 7 nA, and with molecular hydrogen in the background and trapped in the STM junction to enhance spatial resolution.

higher-energy stretch vibrations of an ensemble of molecules on metal surfaces [35,36]. In our study, the two low-frequency vibrations (6.9 ± 0.2 and 2.7 ± 0.3 THz) are within the copper phonon bands that reach a maximum of 7.2 THz for the longitudinal mode along the [001] direction [37]. The energy transfer to induce structural transitions and the efficient coupling to substrate phonons would contribute to the faster vibrational decay.

The structural transition of pyrrolidine can be excited in the absence of light by incoherent tunneling electrons in the STM [34]. In the present study, the cw laser-induced structural transitions are also driven by incoherent hot electrons that can induce chemistry through electronic excitation and electron-vibrational coupling [38]. Excitation by femtosecond laser pulses similarly leads to a constant background of incoherent structural transition rate R_{inc} due to photogenerated hot carriers. However, the novel coherent transition rate R_{coh} is associated with the oscillatory signal that modulates the total rate by 10–15% and decreases as the coherent vibrations decay. When the two pulses overlap in space and time within ±100 fs of the zero delay, the structural transition rate R_{Gauss} exhibits an interference pattern of the electric fields of the two laser pulses and is fitted with a Gaussian envelope. Within the laser pulse width, the structural transitions are likely induced by the light-plasmon polariton within the nanocavity of the STM.

The femtosecond laser operates at a central wavelength of 820 nm, 25 nm bandwidth (46 meV energy spread), and has a 35 fs pulse width that is shorter than the period of the observed oscillations. Therefore, the laser pulses can excite a superposition of the ground and first excited states of low-energy vibrations by impulsive stimulated Raman scattering [39]. The vibrational states would have an oscillatory behavior at a frequency given by the energy difference between the $v = 0$ and $v = 1$ states, which has long been observed in liquids [40].

A deeper understanding of the structural transition for a single pyrrolidine on Cu(001) has been obtained from density functional theory (DFT) calculations, and the technical details are described in Supplemental Material [23]. For state I, eight normal vibrational modes are identified with energies less than 50 meV, as shown in Figs. 3(a)–3(h) and by two videos of the eigenvectors in Supplemental Material. The dominant 6.9 ± 0.2 THz (28.5 meV) oscillation in Fig. 2(b) can be assigned to the mode in Fig. 3(g) (27.2 meV), corresponding to an overall bending motion which lies along the reaction coordinate for the structural transition between the two states. Each laser pulse can coherently excite a superposition of the ground and first excited state of this vibration. The vibrational frequency and time-dependent population of the $v = 1$ state influence the preexponential factor (attempt frequency) in the Arrhenius rate law. The

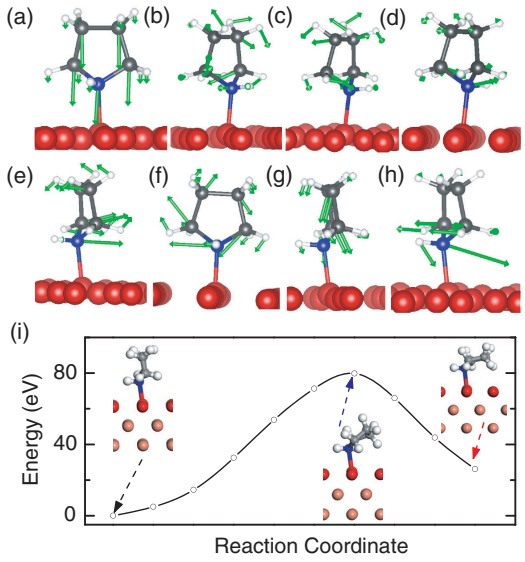

FIG. 3. (a)-(h) DFT calculations of the eight vibrations of a single pyrrolidine adsorbed as state I on the Cu(001) surface with energies smaller than 50 meV (11.85, 12.91, 13.36, 13.57, 17.32, 18.85, 27.24, and 46.51 meV). Green arrows show the directions and amplitudes of atom motions for each eigenmode. Mode a (11.85 meV) and mode g (27.24 meV) are assigned to the two peaks in Fig. 2(b). (i) Energetics pathway for structural transition and the optimized structures for conformations I and II and the transition state between them.

laser pulses excite the molecular vibrations through impulsive stimulated Raman scattering. An increase in the preexponential factor would lead to a higher switching rate. DFT calculations in Fig. 3(i) reveal a difference of 26 meV between the binding energies of state I (0.639 eV) and state II (0.613 eV) and an energy barrier of 79 meV in between. We may also assign the weaker 2.7 ± 0.3 THz (11.3 ± 1.4 meV) oscillation in Fig. 2(b) to the mode in Fig. 3(a) (11.8 meV) that involves the bouncing of the molecule against the surface. Apparently, the periodic variations of the molecule-substrate interaction may modify the activation energy of this structural transition and change the switching rate. The observed oscillations in the transition rate in Fig. 2(a) arise from the corresponding oscillations in the $v = 1$ state from a superposition of the $v = 0$ and $v = 1$ states excited by the first pulse of the pair of phase-correlated laser pulses. The second pulse further excited the molecule from $v = 1$ to higher-energy states above the reaction barrier for the reversible conformational transitions.

The STM allows assessment of the environment on the dynamics of the molecular structural transition. Molecules adsorb in different configurations on the surface and vary in the transition rate, as shown in Fig. 1(e) for a monomer versus a dimer. Besides exhibiting a nearly 70% increase in the transition rate compared to the monomer, the decay time of the coherent oscillations decreases from 1.30 ± 0.17 to 0.90 ± 0.16 ps in Fig. 4(a) for the dimer with an intermolecular separation of 7.21 Å. The decrease of the decay time is attributed to the opening of additional energy transfer channels because of the proximity of another molecule. The presence of intermolecular interactions causes the dominant oscillatory frequency from the FFT spectrum in

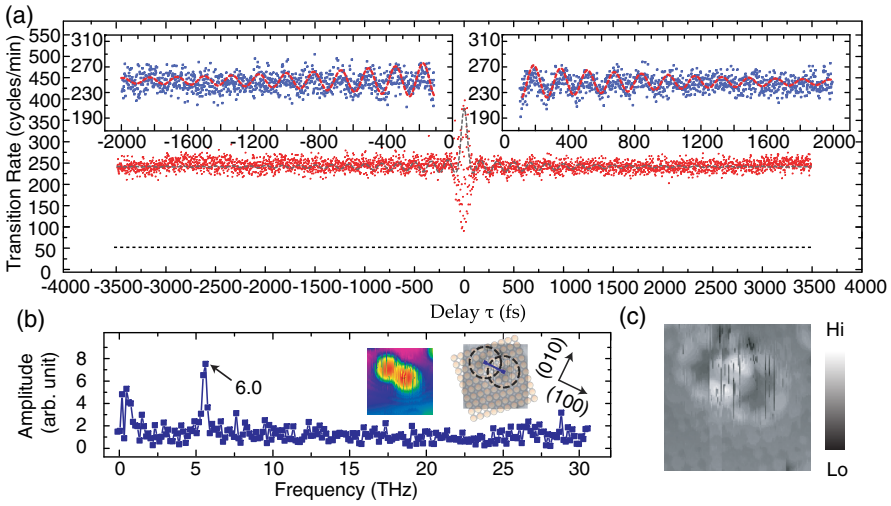

FIG. 4. (a) Delay scan over the center of the lower pyrrolidine molecule separated by 7.21 Å from the upper molecule (red dots), taken under the same conditions as Fig. 2(a). The black dashed line is the fit using Eq. (1). The insets are delay scans taken under the same conditions as the insets in Fig. 2(a). The horizontal dashed line indicates the transition rate vs delay recorded in the dark, as a control measurement, over the same molecule in the dimer, showing a background count rate of ~51 counts min^{-1} driven by tunneling electrons. (b) Fourier transform of time domain data in (a), revealing one peak at 6.0 ± 0.2 THz (167 ± 4 fs or 24.8 ± 0.6 meV; uncertainty obtained from the sinusoidal fit to the delay scan). The insets are a topographic image (left) and an atom-resolved topographic image with a superimposed schematic of substrate surface atoms (right). (c) Atom-resolved topographic image. The smaller white solid circles in a square arrangement are copper atoms of the Cu(001) surface.

Fig. 4(b) to downshift from 6.9 ± 0.2 to 6.0 ± 0.2 THz (24.8 ± 0.6 meV). No other peaks are resolved. The center of each molecule in the dimer coincides with a substrate surface atom [Fig. 4(c)].

The observed oscillations in the structural transition rate in a single pyrrolidine molecule is visualized by the STM and driven by specific vibrations coherently excited by femtosecond laser pulses. The present approach with joint Å-fs resolution can be applied to determine the effects on the structural transition dynamics by substituting different functional groups in the cyclic ring of pyrrolidine. Extensions to other transformations such as reversible proton motions, hindered rotations and diffusion, and conformational change in larger molecules would lead to a broader impact in chemistry through direct visualization in joint space-time.

This work is supported by the National Science Foundation Center for Chemical Innovation on Chemistry at the Space-Time Limit (CaSTL) under Grant No. CHE-1414466. In addition, J. L. was supported by the National Science Foundation of China under Grant No. 11474056.

*To whom all correspondence should be addressed.
wilsonho@uci.edu
†wur@uci.edu

[1] A. H. Zewail, J. Phys. Chem. A **104**, 5660 (2000).
[2] X. Xie *et al.*, Phys. Rev. Lett. **109**, 243001 (2012).
[3] H. Rabitz, R. de Vivie-Riedle, M. Motzkus, and K. Kompa, Science **288**, 824 (2000).
[4] L. Piatkowski, N. Accanto, and N. F. van Hulst, ACS Photonics **3**, 1401 (2016).
[5] G. C. Cho, W. Kütt, and H. Kurz, Phys. Rev. Lett. **65**, 764 (1990).
[6] T. K. Cheng, S. D. Brorson, A. S. Kazeroonian, J. S. Moodera, G. Dresselhaus, M. S. Dresselhaus, and E. P. Ippen, Appl. Phys. Lett. **57**, 1004 (1990).
[7] Y. M. Chang, L. Xu, and H. W. K. Tom, Phys. Rev. Lett. **78**, 4649 (1997).
[8] D. Star, T. Kikteva, and G. W. Leach, J. Chem. Phys. **111**, 14 (1999).
[9] A. N. Bordenyuk, H. Jayathilake, and A. V. Benderskii, J. Phys. Chem. B **109**, 15941 (2005).
[10] K. Watanabe, N. Takagi, and Y. Matsumoto, Chem. Phys. Lett. **366**, 606 (2002).
[11] U. Höfer, I. L. Shumay, C. Reuß, U. Thomann, W. Wallauer, and T. Fauster, Science **277**, 1480 (1997).
[12] W. E. Moerner and L. Kador, Phys. Rev. Lett. **62**, 2535 (1989).
[13] M. Orrit and J. Bernard, Phys. Rev. Lett. **65**, 2716 (1990).
[14] S. W. Hell and J. Wichmann, Opt. Lett. **19**, 780 (1994).
[15] E. Betzig, G. H. Patterson, R. Sougrat, O. W. Lindwasser, S. Olenych, J. S. Bonifacino, M. W. Davidson, J. Lippincott-Schwartz, and H. F. Hess, Science **313**, 1642 (2006).
[16] D. W. Pohl, W. Denk, and M. Lanz, Appl. Phys. Lett. **44**, 651 (1984).
[17] E. Betzig, M. Isaacson, and A. Lewis, Appl. Phys. Lett. **51**, 2088 (1987).
[18] E. Betzig, J. K. Trautman, T. D. Harris, J. S. Weiner, and R. L. Kostelak, Science **251**, 1468 (1991).
[19] S. W. Wu, N. Ogawa, and W. Ho, Science **312**, 1362 (2006).
[20] S. W. Wu and W. Ho, Phys. Rev. B **82**, 085444 (2010).
[21] S. Yoshida, Y. Aizawa, Z.-H. Wang, R. Oshima, Y. Mera, E. Matsuyama, H. Oigawa, O. Takeuchi, and H. Shigekawa, Nat. Nanotechnol. **9**, 588 (2014).
[22] T. L. Cocker, D. Peller, P. Yu, J. Repp, and R. Huber, Nature (London) **539**, 263 (2016).
[23] See Supplemental Material at http://link.aps.org/supplemental/10.1103/PhysRevLett.119.176002 for details of the experiment and DFT methods, supplemental text and figures, and two videos, which includes Refs. [19,20, 24–33].
[24] J. A. Gupta, C. P. Lutz, A. J. Heinrich, and D. M. Eigler, Phys. Rev. B **71**, 115416 (2005).
[25] C. Weiss, C. Wagner, C. Kleimann, M. Rohlfing, F. S. Tautz, and R. Temirov, Phys. Rev. Lett. **105**, 086103 (2010).
[26] S. Li, A. Yu, F. Toledo, Z. Han, H. Wang, H. Y. He, R. Wu, and W. Ho, Phys. Rev. Lett. **111**, 146102 (2013).
[27] C. Weiss, C. Wagner, R. Temirov, and F. S. Tautz, J. Am. Chem. Soc. **132**, 11864 (2010).
[28] A. Yu, S. Li, B. Dhital, H. P. Lu, and W. Ho, J. Phys. Chem. C **120**, 21099 (2016).
[29] R. Temirov, S. Soubatch, O Neucheva, A. C. Lassise, and F. S. Tautz, New J. Phys. **10**, 053012 (2008).
[30] H. Wang, S. Li, H. He, A. Yu, F. Toledo, Z. Han, W. Ho, and R. Wu, J. Phys. Chem. Lett. **6**, 3453 (2015).
[31] B. C. Stipe, M. A. Rezaei, and W. Ho, Rev. Sci. Instrum. **70**, 137 (1999).
[32] B. C. Stipe, M. A. Rezaei, and W. Ho, Science **280**, 1732 (1998).
[33] L. J. Lauhon and W. Ho, J. Chem. Phys. **111**, 5633 (1999).
[34] J. Gaudioso, L. J. Lauhon, and W. Ho, Phys. Rev. Lett. **85**, 1918 (2000).
[35] A. L. Harris, L. Rothberg, L. H. Dubois, N. J. Levinos, and L. Dhar, Phys. Rev. Lett. **64**, 2086 (1990).
[36] M. Morin, N. J. Levinos, and A. L. Harris, J. Chem. Phys. **96**, 3950 (1992).
[37] E. C. Svensson, B. N. Brockhouse, and J. M. Rowe, Phys. Rev. **155**, 619 (1967).
[38] *Laser Spectroscopy and Photochemistry on Metal Surfaces, Part I and Part II*, edited by H.-L. Dai and W. Ho (World Scientific, Singapore, 1995).
[39] S. Ruhman, A. G. Joly, and K. A. Nelson, J. Chem. Phys. **86**, 6563 (1987).
[40] M. J. Rosker, F. W. Wise, and C. L. Tang, Phys. Rev. Lett. **57**, 321 (1986).